

A COMPARISON OF SINGLE-CYCLE VERSUS MULTI-CYCLE
PROOF TESTING STRATEGIES

Stephen J. Hudak, Jr.

Department of Materials Sciences

Southwest Research Institute

San Antonio, TX 78284

and

Dale A. Russell

Rocketdyne Division

Rockwell International

Canoga Park, CA 91303

ABSTRACT

Proof testing has been a useful supplement to conventional nondestructive evaluation (NDE) of space shuttle main engine (SSME) components. Since many of these components involve thin sections and high toughness materials, such as Inconel 718, conventional single-cycle proof test logic is not applicable due to the propensity for stable crack growth during the proof test. The purpose of this paper is to summarize experience with five-cycle proof testing of SSME components and outline a framework for understanding multi-cycle proof testing using the fracture mechanics concept of a resistance curve. Extreme value statistics are also used to propose an empirical approach to compare the advantages and disadvantages of single- versus multi-cycle proof testing. The importance of the initial flaw size distribution and specimen thickness in such a comparison is also discussed.

1. Introduction

Although proof testing is generally not the preferred method of crack detection, it has proven useful as a supplement to conventional nondestructive evaluation (NDE) methods, particularly when NDE is compromised by geometric complexities of the component, or structure. The objective of proof testing is to screen out gross manufacturing or material deficiencies and therefore provide additional quality assurance of delivered hardware. It is in this spirit that Rocketdyne has utilized proof testing on components of the Space Shuttle Main Engine (SSME). In this case, Rocketdyne has applied a modified version of conventional single-cycle proof testing which involves multi-cycle testing. Based on demonstrated success on a number of propulsion systems over the years, five-cycle proof testing has been adopted as the standard. Testing typically occurs prior to service, although in special cases it could also be utilized as part of an in-service inspection.

Potential benefits of proof testing must always be weighed against the possibility of inflicting additional undetected damage on the component through subcritical crack growth on loading. The decision as to whether or not to use proof testing for the purpose of flaw screening, as well as the development of an optimum strategy for such testing, requires appropriate fracture mechanics analysis. Since the application of proof testing to brittle materials results in little or no stable crack growth on loading, multi-cycle proof testing is unnecessary and the relevant fracture mechanics analysis is relatively straightforward. On the other hand, multi-cycle proof testing is applicable to tougher materials which often exhibit significant stable crack growth on loading and the relevant fracture mechanics analysis can be considerably more complex. Although these techniques have been outlined [1,2], certain underlying concepts remain unproven and the appropriate fracture mechanics material properties, needed to characterize the propensity for stable crack growth, are generally not available.

Southwest Research Institute is presently conducting an experimental research program whose objective is to define the relative advantages and disadvantages of single versus multi-cycle proof testing [3]. Although experimental results are not yet available from this program, the intent of this paper is to define the problem and identify the underlying factors which will control the outcome of such a comparison. First, Rocketdyne's experience with five-cycle proof testing is briefly summarized, then the strategies of single- and multi-cycle proof testing are outlined and discussed within the context of the generalized concept of a crack growth resistance curve.

2. Summary of Multi-Cycle Proof Testing Experience

Multi-cycle proof testing of pressurized components has been selectively implemented by Rocketdyne since 1952. It originated as the result of components failing at pressures significantly less than those used in successful hydrostatic proof testing. The current procedure for multi-cycle proof testing on the SSME consists of the application of five proof cycles at a minimum pressure of 1.2 times the maximum operating pressure, each with a hold time of approximately 30 seconds. The proof pressure is typically selected to keep nominal stresses below 85% of the material's ultimate strength; although this stress level is low enough to preclude generalized yielding, localized yielding can sometimes occur.

The primary justification for five-cycle proof testing is the successful record of performance of Rocketdyne engines and lack of

service failures of pressurized components whenever this procedure has been implemented. This experience, summarized in Table 1, includes cases where components have passed the first cycle of pressurization of a five-cycle proof test only to fail on a subsequent proof pressure cycle at or below full pressure. As indicated, many of these cases involved components of the SSME where hardware deficiencies, judged to present a significant risk of catastrophic failure in service, were revealed after having passed the first proof pressure cycle. As one might expect, the highest incidence of proof test failures has occurred in components with the lowest design margin.

While not clearly evident from the comments in Table 1, it is significant to note that many of the components listed contain relatively thin sections. This observation is consistent with a propensity for thin sections to exhibit stable crack growth on loading as discussed in Section 4 in terms of R-curve behavior.

3. Single Cycle Proof Testing Strategy

The philosophy underlying single cycle proof testing has been adequately established; for example, see the work of Tiffany [4]. Perhaps the most well known example of the successful application of proof testing is that of the low temperature testing of the F-111 wing box at McClellan Air Force Base [5].

As a prelude to understanding multi-cycle proof testing, let us first consider the basic concept of single cycle proof testing of a material under brittle conditions. This can best be accomplished by examining Figure 1 which illustrates conventional proof testing logic in terms of both the residual strength (σ_r), as well as residual fatigue life (N_f) of a structural component. As indicated, the proof test stress (σ_p) is selected to be some fraction of the material's ultimate strength (σ_{ult}) such that gross deformation of the structure is avoided, although local yielding may occur at geometric stress concentrations. Since brittle materials exhibit a well-defined instability point given by $K_{max} = K_{Ic}$, the successful application of σ_p guarantees that any flaw that may be present is less than some size, a_i . Using a_i as the initial crack size in a fracture mechanics based fatigue crack growth analysis defines a corresponding initial residual fatigue life, N_i . Provided periodic proof testing can reliably ensure that the maximum crack size remains below a_i , its use during service offers the opportunity to extend the life of the component. The interval $a_f - a_i$ defines the crack size regime over which periodic proof testing at σ_p will result in crack detection through proof failure thereby removing the component from service before the critical flaw size, a_f , is reached.

TABLE 1

SUMMARY OF ROCKETDYNE'S EXPERIENCE WITH FIVE-CYCLE PROOF TESTS WHICH FAILED ON OTHER THAN THE FIRST CYCLE (Period: 1973 - 1979)

Program	Component	Material at Failure Location	Failure Cycle	Proof Pressure at Failure
SSME	LPOTP Housing	TENS-50	4th	80%
	Nozzle Tee	Inco 718 Weld	2nd	
	Nozzle Mixer Bowl	Inco 718 Casting	1st to 3rd	Leakage
	HPOTP Bellows Assy		N/A	100%
	Turbine Discharge Duct Bellows Assy	Inco 718	2nd	56%
	HPOTP Bellows		N/A	100%
	Main Injector	Inco 718 EB Weld	2nd	100%
	High-pressure Fuel Duct	SA1-2.5Sn Ti Weld HAZ	4th (cryo)	100%
	Fuel Turb. Drive Duct	Inco 718	2nd	75%
	Low Pressure Oxidizer Duct Flex Joint	Inco 718 Heat Treated Weld	1st (cryo)	100% "pop" sound at 70%
	Oxid. Tank Pressurant "Short" Bellows (2 incidents)	Inco 718 wrought	4th 2nd	100%
	Powerhead Preburner Fuel Supply Duct	Alloy 903	5th	100%
	Flight Nozzle Tubes	A-286	Numerous occurrences on 2 to 5 cycles	Various pressure levels
	HPOTP Inlet	SA1-2.5Sn Ti Weld HAZ	3rd (ambient)	100%

(Continued on Next Page)

TABLE 1 (CONTINUED)

SUMMARY OF ROCKETDYNE'S EXPERIENCE WITH FIVE-CYCLE PROOF TESTS
WHICH FAILED ON OTHER THAN THE FIRST CYCLE (Period: 1973-1979)

Program	Component	Material at Failure Location	Failure Cycle	Proof Pressure at Failure
Nelar	Helium Bottle	4130 Bar Heat Treat 180-200 ksi	See Comments	See Comments
Thor	Gas Generator Blade Valve Housing	356-T6 Al Casting	5th	78%
Atlas MA-5	Turbine Inlet Manifold Nut	300 Series CRES	3rd	100%
F-1	Thrust Chamber Tubes	Inconel X-750	3rd	61%
F-1	MK-10 Fuel Volute Casting	Tens 50-T60 Casting	5th	During De- pressurization from 100%
RS-27	Turbopump Fuel Inlet Elbow (4 Incidents)	6061 Al Weld	2nd	100%

ORIGINAL PAGE IS
OF POOR QUALITY

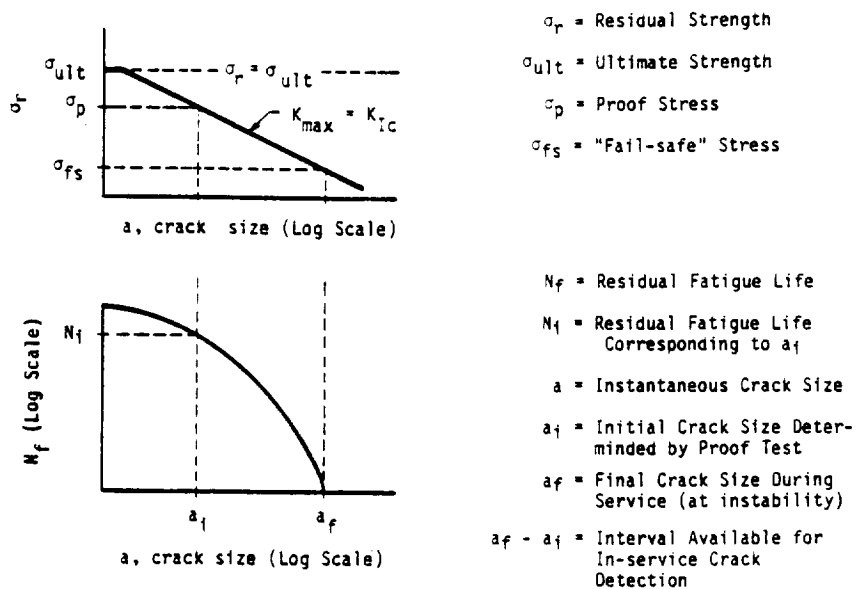


FIGURE 1. Single-cycle proof stress logic represented in terms of residual strength and residual fatigue life.

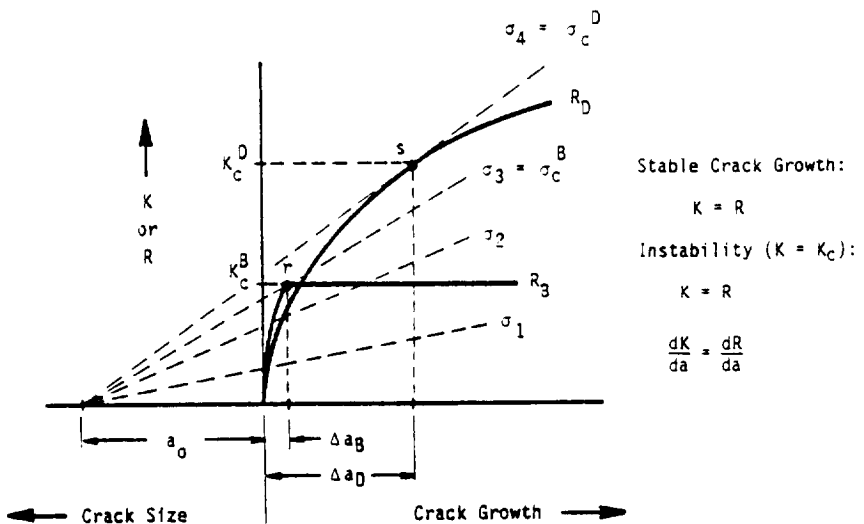


FIGURE 2. Influence of R-curve on maximum extent of stable crack growth in "Brittle" ('B') versus "Ductile" ('D') materials.

Although the foregoing discussion uses the term "brittle material", it is important to recognize that whether or not a material exhibits brittle behavior is dependent upon geometric constraint and loading rate, as well as test temperature. In fact the temperature dependence of the material can be used to advantage in designing the proof test. Specifically, for materials in which K_{Ic}/σ_{ys} is significantly reduced as temperature is decreased, σ_p/σ_{ys} can be reduced by performing the proof test at a temperature lower than the operating temperature. This strategy was used in the case of the F-111 proof testing [5], and more recently in the case of cryogenic proof testing of titanium disks in the Air Force's F-100 engines in F-15 and F-16 fighter aircraft.

4. Multi-Cycle Proof Testing Strategy and the R-Curve Concept

There is no advantage to multi-cycle proof testing in materials which behave in a brittle fashion since significant stable crack growth on loading does not occur. However, multi-cycle proof testing appears to offer distinct advantages in materials which behave in ductile fashion, as demonstrated by Rocketdyne's experiences which are summarized in Section 2. The success of multi-cycle proof testing is believed to be due to the occurrence of stable crack growth on loading. In general, this phenomenon is dependent on a variety of factors--including stress state, temperature and material condition--and can best be understood in terms of resistance curve concepts.

The general concept of a resistance curve is attributable to Krafft [6] and involves an energy balance between the driving force for crack growth and the inherent resistance to crack growth of the material. Subsequently, McCabe and co-workers (e.g., see Ref. [7]) popularized the approach and developed standard methods for measuring R-Curves under linear elastic conditions. The approach has also been shown to apply to cyclic loading [8,9]; thus, its use is compatible with a conventional fracture mechanics approach to fatigue crack growth. More recently, the resistance curve concept has been extended to fracture under elastic-plastic loading [10,11] using the J-integral [12]. The latter has been formalized by Paris and co-workers [13,14] into the tearing instability approach. Thus, the resistance curve concept is applicable to a variety of failure modes and loading conditions, including stable crack growth within highly deformed regions at geometric stress concentrations [15]. However, for simplicity, the following discussion relating resistance curve concepts and multi-cycle proof testing is presented within the framework of linear elastic fracture mechanics.

As illustrated in Figure 2, the resistance curve concept can best be understood by considering both the driving force (K) and material resistance (R)* as functions of the extent of stable crack growth, Δa , which occurs during loading. Here the resistance curve, or R-curve, is compared for two materials: the brittle material exhibits a relatively flat R-curve (R_B), while that for the ductile material (R_D) rises steeply as the crack extends. The marked increase in the R-curve in the latter case is believed to be associated with the formation of shear lips near the surface of the specimen, reflecting the influence of a relative change in crack-tip stress state from plane strain to plane stress as the specimen surface is approached. The dashed lines emanating from a common point are the superimposed driving forces for increasing values of applied nominal stress σ_1 through σ_4 . Although stable crack growth can occur when $K = R$, the onset of crack instability does not occur until both: $K = R$ and $\partial K / \partial a = \partial R / \partial a$. Because of the flatness of the R-curve in the case of the brittle material, these conditions can only be met at point r , for an applied stress σ_3 . Thus, σ_3 is a critical stress, designated σ_c^B , and provided the extent of prior crack growth (Δa_B) is small, this corresponds to K_{Ic} . In contrast, for the case of ductile materials, instability occurs at point s , corresponding to a critical stress σ_c^D , and toughness K_c^D . As a consequence of differences in the nature of the R-curve, both the toughness and the extent of crack extension prior to instability can differ significantly. Moreover, contrary to the case of the brittle material, the value of apparent toughness for the ductile material is not unique, as will be discussed below.

For example, Figure 3 schematically shows how the character of the R-curve changes as a function of specimen (or component) thickness. Consequently, even for a fixed material, specimen geometry, and initial crack size, the toughness is seen to systematically increase with decreasing thickness, B . Moreover, altering the planar geometry such that the applied K varies, as shown in Figure 4, causes the toughness and extent of stable crack growth (Δa_1 versus Δa_2) to change significantly, even though the material and initial crack size are held constant. Finally, even for a constant planar geometry, thickness, and material, the apparent toughness (K_c) can vary with initial crack size, as a result of crack resistance development during stable crack growth as shown in Figure 5.

* Under linear elastic loading, the materials resistance is also commonly referred to as K_R , but R will be used here for clarity.

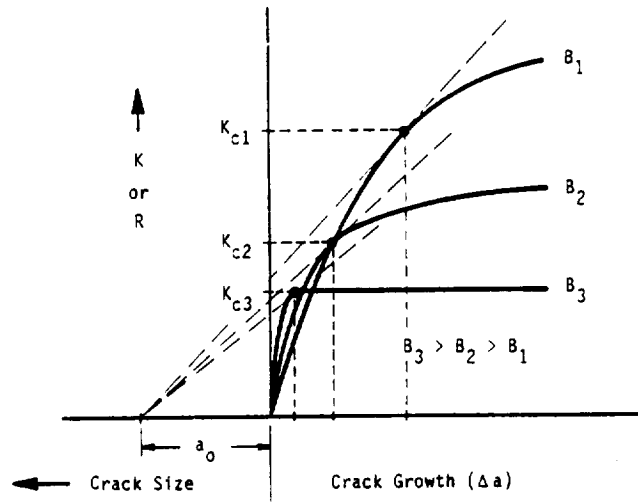


FIGURE 3. Influence of component thickness (B) on fracture toughness (K_C) and extent of crack growth (Δa) for a given material condition and initial crack size (a_0).

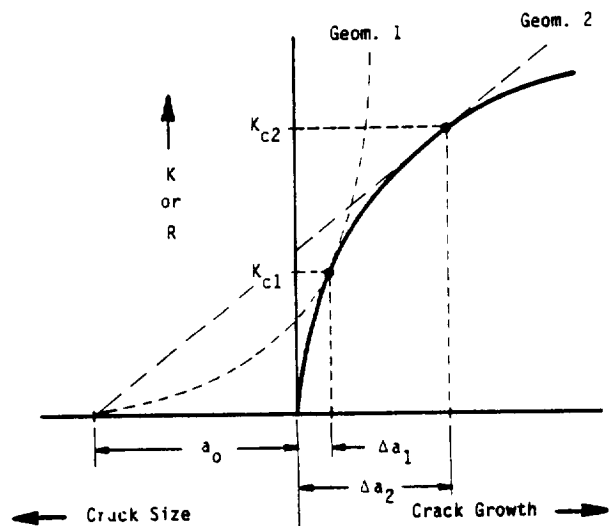


FIGURE 4. Influence of component geometry on the fracture toughness (K_C) and extent of crack growth (Δa) for a given material and initial crack size (a_0).

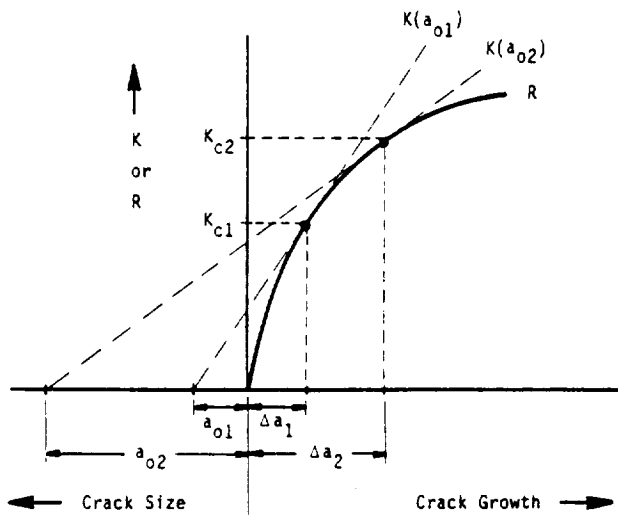


FIGURE 5. Influence of initial crack size (a_0) on the fracture toughness (K_C) and extent of crack growth (Δa) in a given material and geometry.

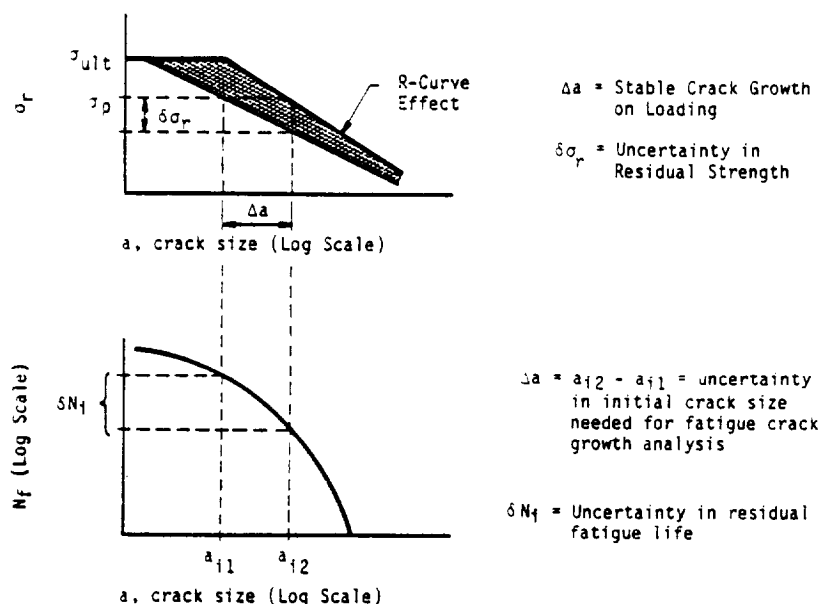


FIGURE 6. Uncertainty in residual strength and residual fatigue life due to stable crack growth on loading during the proof test of "ductile" materials.

Thus, we can summarize the differences between brittle and ductile material response as follows:

a) Brittle Response (Low toughness and thick sections):

1. R-Curve: Flat
2. Stable Crack Growth: little or none
3. Instability Condition: $K = K_{Ic}$

b) Ductile Response (High toughness and thin sections):

1. R-Curve: Steep
2. Stable Crack Growth: can be extensive
3. Instability Condition: $K = R$ and $\partial K / \partial a = \partial R / \partial a$;
4. Apparent toughness: $K_c = K_c(B, a_o, \text{ and Geom.})$

It follows from the above conditions that brittle materials have a straightforward proof test logic as summarized previously in Figure 1. In contrast, the propensity for stable crack growth and more complex instability conditions of ductile materials give rise to the less certain proof test logic of Figure 6. Here stable crack growth on loading (Δa), due to the R-curve effect, produces uncertainty in the residual strength (δS_r), as well as in the residual fatigue life (δN_f).

In theory the above uncertainty can be eliminated through the proper application of R-Curve concepts [1], although this has not yet been demonstrated quantitatively, nor have the relevant R-curve data been generated, especially for surface and embedded defects.

Based on the above discussion, it is clear that the character of the material's resistance curve holds the key to proper selection of an optimum proof test strategy. Materials which are either inherently tough (Figure 2), or are used in thin sections (Figure 3), are well suited for multi-cycle proof testing. Conversely, materials with inherently low toughness, or those subjected to high degrees of geometric constraint, are well suited for single-cycle proof testing. Since Inconel 718, the primary structural material in the SSME exhibits high toughness, it is concluded that component thickness and flaw geometry are the primary geometric variables controlling the selection of an optimum proof test strategy. As mentioned previously, this is consistent with Rocketdyne's five-cycle proof testing experience (Section 2).

5. Key Factors in Comparison of Single Versus Multi-Cycle Proof Testing

A number of factors have been considered to ensure the proper design of experiments comparing single versus multi-cycle proof testing in Ref. [3]. The R-curve concepts discussed in the previous sections provide guidance on the proper selection of variables so that results are not unduly biased toward either one of these procedures. Specifically, it follows from the influence of thickness on the propensity for stable crack growth (Figure 3) that thick specimens will favor single-cycle proof testing, while thin specimens will tend to favor multi-cycle proof testing. Thus, the experimental design being utilized in Ref. [3] provides for a comparison of data at various thicknesses which are typical of those used in SSME components.

The distribution of initial crack sizes in the experimental comparison has also been a key consideration. This is particularly true at the upper tail of the crack size distribution where the behavior of the larger defects will result in the most dramatic differences between the two procedures, specifically, where either of the following events will occur: 1) survival of large initial cracks during the proof test will cause short fatigue lives, and 2) growth and instability of large initial cracks during proof testing will cause their removal from the population of fatigue lives. Thus, the experimental design in Ref. [1] has been approached as a problem in extreme value statistics. This approach is consistent with the philosophy of proof testing--that is, to eliminate the unusually large defect which, having escaped detection during nondestructive inspection, causes an unacceptably low fatigue life.

In order to ensure that the results are applicable to SSME components, initial flaw size distributions are being derived based on data from SSME components, as well as welded IN 718 coupon tests. Preliminary results suggest that these initial flaw sizes can be represented by either Weibull or lognormal distributions. An initial flaw size distribution of this general type is schematically shown in Figure 7, where it is compared with anticipated alterations resulting from either single- or multi-cycle proof testing. As indicated, the single-cycle proof testing may increase the number of large cracks, due to stable crack growth, while eliminating a relatively few cracks from the entire population. On the other hand, the multi-cycle proof testing is expected to increase the size of a greater number of cracks, while eliminating the largest cracks from the total population. This anticipated result is schematically illustrated using the R-curve in Figure 8 which is assumed to be invariant from cycle-to-

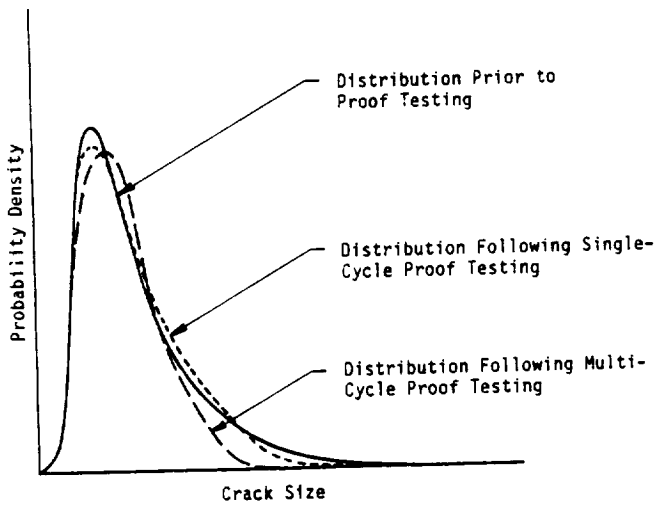


FIGURE 7. Schematic illustration of anticipated changes in crack size distribution following single and multi-cycle proof testing.

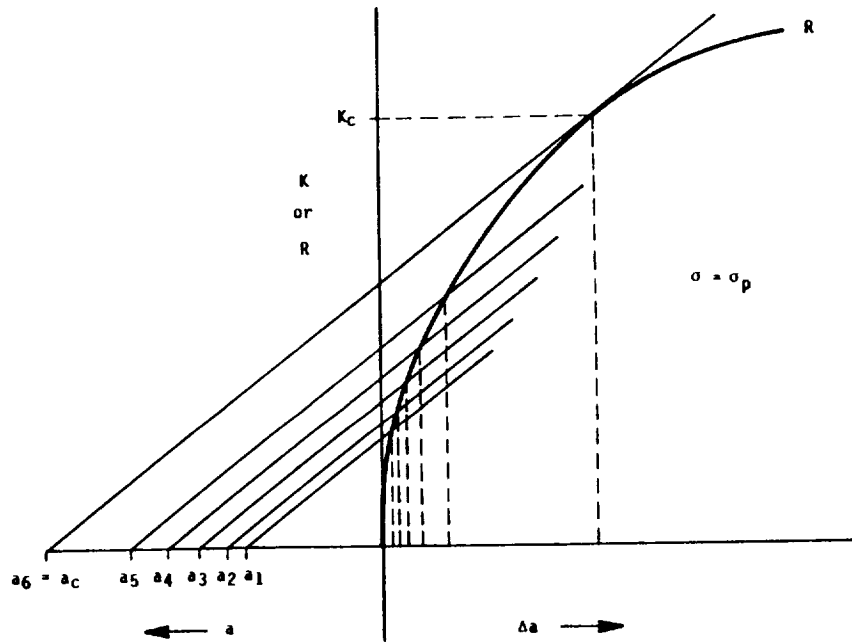


FIGURE 8. Stable crack extension during proof testing illustrating the influence of the number of proof cycles on the extent of crack growth (Δa) and the post-proof flaw distribution.

cycle. As indicated, an initial flaw size, a_1 , will grow in stable fashion on sequential cycles to a_2 , a_3 , a_4 , and a_5 , until the onset of instability of a_6 on the sixth cycle. Thus, five-cycle proof tests on components containing a distribution of initial flaw sizes between a_1 and a_6 will result in failures for all flaws greater than a_2 . These eliminated flaw sizes will be replaced by flaws which were initially between a_1 and a_2 . In contrast, during single-cycle proof testing each flaw in this same initial distribution will enlarge by one crack growth increment and only flaws greater than a_6 will be eliminated by virtue of their failure. Consequently, fewer large flaws are expected to remain following five-cycle proof testing than after single-cycle proof testing.

It is clear that the most significant differences introduced by the two types of proof testing will occur in the upper tail of the crack size distribution. These differences will translate into the lower tails (minimum lives) of the fatigue life distributions. In other words, the behavior of the flaws which just barely escape detection in either proof test will be critical in controlling the statistics of the subsequent fatigue tests. Thus, if crack sizes are apportioned in the experiments either uniformly or even from the entire distribution curve, there is a risk of losing valuable information. Such dilution is likely to provide little information in the upper tail of the crack size distribution and lower tail of the fatigue life distribution. Consequently, to avoid such problems, the experiments in Ref. [3] are concentrating on the crack sizes in the upper tail of the distribution.

In addition to the statistical soundness of the above approach, it is also consistent with the design philosophy of the SSME. The SSME was designed for 240 flights, but its anticipated mission use is only 55 flights and 5 tests, thus a safety factor of four on life was used. In view of this general conservatism, the primary role of proof testing of SSME components is to eliminate the atypical, large defects which occasionally escape NDE. Since these defects are contained in the upper end of the distribution curve, it is appropriate to emphasize these extreme values in comparing the two proof test methods. This approach will enable several specimen thicknesses to be examined without compromising the robustness of the statistical analysis.

Figure 8 also illustrates that the large differences in the extent of crack extension for flaws of different sizes will result in a law of diminishing returns. Thus an optimum number of proof cycles is expected to occur. However, this optimum number will depend on the character of the material's resistance curve, the geometry of the component, as well as the initial flaw size distribution. The

development of a component-specific optimum proof testing strategy will depend on establishing a reliable initial flaw size distribution, which may depend on the details of weld fabrication. In addition, in order to quantify the previously presented concepts, several technical challenges associated with the characterization of stable crack growth of surface flaws will need to be addressed. These include both experimental and analytical difficulties arising from three-dimensional, variable-constraint effects, as well as elastic-plastic crack growth.

6. Acknowledgment

This paper is based on the initial phase of work under NASA Contract No. NAJ8-37451. Mr. Larry Salter is the NASA/MJFC technical project manager.

7. References

1. J. Mendoza and G. A. Vroman, "Multiple Cycle Proof Test Logic," Rocketdyne Internal Report SSME 73-410, Pub 572-K-9, 20 December 1973.
2. P. M. Besuner, D. O. Harris, and J. M. Thomas, "A Review of Fracture Mechanics Life Technology," NASA Contractor Report 3957, February 1986.
3. "Comparison of Single- Versus Multiple-Cycle Proof Testing," NASA/MSFC Contract NAS8-37451, Southwest Research Institute, San Antonio, TX.
4. E. F. Tiffany and J. H. Masters, "Applied Fracture Mechanics," Fracture Toughness Testing and Its Applications, ASTM STP 381, 1965.
5. W. D. Buntin, "Concept and Conduct of Proof Testing of F-111 Production Aircraft," Aeronautical Journal, Vol. 76, No. 742, pp. 587-598, 1972.
6. J. M. Krafft, A. M. Sullivan, and R. W. Boyle, "Effect of Dimensions on Fast Fracture Instability of Notched Sheets," Proc. of the Crack Propagation Symposium, Cranfield, England, Vol. 1, 1961, pp. 8-26.
7. Fracture Toughness Evaluation by R-Curve Methods, ASTM STP 527, American Society for Testing and Materials, 1973.

8. D. P. Wilhem and M. M. Ratwani, "Application of the R-Curve Concept to Fatigue Crack Growth," *Trans. ASME, J. of Engr. Matls. and Tech.*, Vol. 100, 1978, pp. 416-420.
9. K.-H. Schwalbe, "Some Properties of Stable Crack Growth," *Engr. Fract. Mech.*, Vol. 11, 1979, pp. 331-342.
10. J. A. Begley and J. D. Landes, "The J-Integral as a Fracture Criterion," in Fracture Toughness, Part II, ASTM STP 514, 1972, pp. 1-20.
11. J. D. Landes and J. A. Begley, "The Effect of Specimen Geometry on J_{Ic} ," in Fracture Toughness, Part II, ASTM STP 514, 1972, pp. 25-39.
12. J. R. Rice, "Mathematical Analysis in the Mechanics of Fracture," in Fracture, Vol. 2, Academic Press, N.Y., 1968, pp. 191-311.
13. P. C. Paris, H. Tada, H. Ernst, and A. Zahorr, "Initial Experimental Investigation of Tearing Instability Theory," in Elastic-Plastic Fracture, ASTM STP 668, 1979, pp. 251-265.
14. P. C. Paris, H. Tada, A. Zahorr, and H. Ernst, "Instability of the Tearing Mode of Elastic-Plastic Crack Growth," in Elastic-Plastic Fracture, ASTM STP 668, 1979, pp. 5-36.
15. D. Shows, A. F. Liu, and J. FitzGerald, "Application of Resistance Curves to Crack at a Hole," in Fracture Mechanics: Fourteenth Symposium, Volume II: Testing and Applications, ASTM STP 791, 1983, pp. II-87 - II-100.